Electron–electron interaction effects on the photophysics of metallic single-walled carbon nanotubes

2009 J. Phys.: Condens. Matter 21 095009

(http://iopscience.iop.org/0953-8984/21/9/095009)

J. Phys.: Condens. Matter **21** (2009) 095009 (8pp) doi:10.1088/0953-8984/21/9/095009

Electron–electron interaction effects on the photophysics of metallic single-walled carbon nanotubes

Zhendong Wang, Demetra Psiachos, Roberto F Badilla and Sumit Mazumdar

Department of Physics, University of Arizona, Tucson, AZ 85721, USA

Received 28 October 2008, in final form 26 December 2008
Published 13 February 2009
Online at stacks.iop.org/JPhysCM/21/095009

Abstract

Single-walled carbon nanotubes are strongly correlated systems with large Coulomb repulsion between two electrons occupying the same p_z orbital. Within a molecular Hamiltonian appropriate for correlated π-electron systems, we show that optical excitations polarized parallel to the nanotube axes in the so-called metallic single-walled carbon nanotubes are excitons. Our calculated absolute exciton energies in twelve different metallic single-walled carbon nanotubes, with diameters in the range 0.8–1.4 nm, are in nearly quantitative agreement with experimental results. We have also calculated the absorption spectrum for the (21, 21) single-walled carbon nanotube in the E_{22} region. Our calculated spectrum gives an excellent fit to the experimental absorption spectrum. In all cases our calculated exciton binding energies are only slightly smaller than those of semiconducting nanotubes with comparable diameters, in contradiction to results obtained within the *ab initio* approach, which predicts much smaller binding energies. We ascribe this difference to the difficulty of determining the behavior of systems with strong on-site Coulomb interactions within theories based on the density functional approach. As in the semiconducting nanotubes we predict in the metallic nanotubes a two-photon exciton above the lowest longitudinally polarized exciton that can be detected by ultrafast pump-probe spectroscopy. We also predict a subgap absorption polarized perpendicular to the nanotube axes below the lowest longitudinal exciton, blueshifted from the exact midgap by electron–electron interactions.

1. Introduction

Correlated-electron systems often exhibit behavior that is substantively different from what is expected within one-electron (1-e) theory. In particular, the classification of materials as simple metals or semiconductors breaks down for sufficiently strong electron–electron (e–e) interactions. The effects of e–e interactions are particularly strong in low dimensions, and carbon-based quasi-one-dimensional (quasi-1D) systems such as π-conjugated polymers, semiconducting and conducting charge-transfer solids, and carbon nanotubes commonly exhibit novel behavior ascribed to e–e interactions. Although it is by now generally accepted that Coulomb interactions between the π-electrons are strong in single-walled carbon nanotubes (SWCNTs), they continue to be classified as metallic (M-SWCNTs) and semiconducting (S-SWCNTs), based on the predictions of 1-e theory. Thus, SWCNTs with chirality indices (n, m) are commonly referred to as metallic if $(n - m) = 3j$, where j is an integer including zero, and semiconducting otherwise. Schematic π-electron tight-binding band structures of the armchair ($n = m$) and nonarmchair ($n \neq m$, including $m = 0$) M-SWCNTs are shown in figure 1. The innermost valence and conduction bands (VB and CB, respectively) have linear dispersions and meet at Dirac points, which constitute the Fermi points here. The crossing innermost bands are missing in the S-SWCNTs; otherwise their band structures are similar to those in figure 1(b). We continue to use the nomenclature based on 1-e theory for simplicity in what follows, with the recognition that simple classifications of SWCNTs may not be entirely meaningful.

In recent years, there has been a strong interest in the consequences of e–e interactions on the photophysics of S-SWCNTs. The bulk of the existing literature is on optical absorptions polarized parallel to the NT axes, where e–e interactions lead to exciton formation. The exciton character of

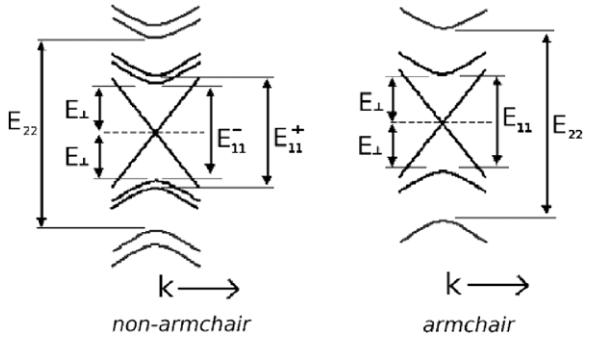

Figure 1. (a) Schematics of the tight-binding band structures of M-SWCNTs and longitudinal and transverse optical transitions within one-electron theory. Splittings due to the trigonal warping are indicated for nonarmchair NTs. The same E_{11} and E_{22} transitions occur in the S-SWCNTs, which do not have inner crossing bands.

the longitudinally polarized absorptions in S-SWCNTs [1–10] is now firmly established. Nonlinear absorption [11] and two-photon-induced fluorescence [12–14] have demonstrated that the binding energy of the lowest longitudinal optical exciton in S-SWCNTs is substantial relative to the optical gap. Research on optical absorptions polarized *perpendicular* to the NT axes has been less extensive [7, 15–18], but the consequences of e–e interactions here are even more dramatic. Within 1-e theory, perpendicularly polarized absorption occurs exactly at the center of the two lowest longitudinally polarized absorptions (hereafter E_{11} and E_{22}, see figure 1). The experimentally observed strong blueshift of the perpendicularly polarized absorption [15] to near E_{22} is due to e–e interactions [7, 16–18].

There also exists a considerable body of theoretical [19–25] and experimental [26–29] literature on the effects of e–e interactions on the M-SWCNTs, which until recently had focused mostly on transport behavior. Screening of the interactions between the π-electrons in these 1D systems is weak and the lowest excitations in M-SWCNTs have been shown to correspond to those of a Luttinger liquid (LL) rather than a Fermi liquid. Indeed, it has been claimed [19] that the lowest excitations within a Hubbard model description of (n, n) armchair M-SWCNTs can be approximately mapped onto those of two-leg 'Hubbard ladders' [30] with an effective on-site Hubbard repulsion $U_{\rm eff} \sim U/n$, where U is the repulsion between two electrons occupying the same p_z carbon orbital. Although excitations in nonarmchair M-SWCNTs are more complex, it is believed that the low energy physics of these are the same as in the armchair tubes. The Hubbard model with only on-site Coulomb interaction is overly simple for carbon-based systems, in which long-range intersite e–e interactions play a strong role. Within models incorporating realistic on-site and intersite e–e interactions, electron correlation effects are strongly structure-dependent. Within such models, for example, linear chain π-conjugated polymers such as polyacetylene behave as Mott–Hubbard semiconductors with strong spin–spin correlations, but related quasi-1D polymers with benzene groups, such as poly(paraphenylene) and poly(paraphenylenevinylene), behave as band semiconductors with relatively small spin–spin correlations but large exciton binding energies [31]. Similar realistic modeling of S-SWCNTs has shown that the lowest triplet excitation in these is only slightly below the optical exciton [32], indicating that the lowest triplet has a strong charged electron–hole character. This, in turn, is a signature of weak spin–spin correlations in SWCNTs. Some evidence for antiferromagnetic spin–spin correlations, nevertheless, has recently been found in M-SWCNTs [33, 34] and carbon nanohorns [35]. The charging energy of a tube is also determined primarily by the long-range component of the e–e interactions, which has also been shown to be weakly screened [20]. Fitting the experimental charging energy of an M-SWCNT [26] with a $1/|x|$ potential, for example, requires a dielectric constant of only 1.4 [20].

It is in this context that we examine theoretically the photophysics of M-SWCNTs here. We are concerned not about the lowest excitations involving the electrons occupying the innermost bands in figure 1, but about optical transitions in the visible region. Electronic transitions leading to optical absorptions within 1-e theory are indicated in figure 1. In addition to the VB-to-CB transitions that are polarized parallel to the NT axes, we expect also midgap transitions polarized perpendicular to the NT axes, based on our experience with S-SWCNTs [7, 17]. Only the absorptions parallel to the NT axis have been experimentally investigated in M-SWCNTs so far [36–40]. In view of the weak screening of the e–e interactions in M-SWCNTs (see above), we expect the 'large Hubbard U' description to be appropriate here, *even if these systems are conducting and are not Mott–Hubbard semiconductors.* Note that, unlike in true 1D, the Hubbard U has to be larger than a critical value before a metal-to-insulator transition will occur in graphene. Conducting behavior thus is not a signature of reduced U. Taken together with the large atomic U scenario, the 1:1 correspondence of the VB-to-CB transitions in figure 1 to those in the S-SWCNTs then suggests that photoexcitations in M-SWCNTs are to excitons with binding energies that are perhaps comparable to those in the S-SWCNTs. This conjecture is, however, in strong contradiction to existing theoretical results [41]. Within the latter method the ground state is determined using an *ab initio* approach, which is followed by the determination of the quasi-particle energies within the GW approximation and the solution of the Bethe–Salpeter equation of the two-particle Green's function. This technique has claimed that binding energies in M-SWCNTs are an order of magnitude smaller than those in S-SWCNTs with comparable diameters. Recent work has also claimed that the experimental E_{22} absorption of the (21, 21) armchair M-SWCNT can be fitted well within the *ab initio* theory, and that the exciton binding energy in this system is only 0.05 eV [40]. The absence of two-photon-induced fluorescence in M-SWCNTs (because of the inner VB and CB) has prevented the direct measurement of exciton binding energies. It then becomes imperative to investigate the photophysics of M-SWCNTs theoretically using other approaches.

In the present paper, we report the results of many-body calculations of the photophysics of M-SWCNTs, based on a molecular Hamiltonian that has previously yielded quantitatively accurate results for the absolute exciton energies,

exciton binding energies and nonlinear absorption in S-SWCNTs [7, 8, 11, 17]. The exciton binding energies we obtain for M-SWCNTs are considerably larger than those found in [41]. In agreement with the earlier LL theories, our results indicate that screening of the electron–hole interactions in M-SWCNTs is considerably weaker than in conventional metals.

In section 2 we present our π-electron Hamiltonian and indicate how the parameters of the Hamiltonian are obtained. We then give a brief justification of the choice of our parameters. In section 3.1 we present our theoretical results for linear and nonlinear absorptions in the M-SWCNTs. Our results for the absolute exciton energies are in excellent agreement with experiments for all twelve M-SWCNTs that we have studied. Our calculated exciton binding energies are much larger than those predicted within the *ab initio* theory. In section 3.2 we compare our calculated absorption spectrum of the (21, 21) M-SWCNT with the experimental spectrum [40]. Again, excellent agreement between the theoretical and experimental absorption spectra is obtained. Finally, in section 3.3 we present our predicted theoretical absorption spectra polarized perpendicular to the NT axes. As with the S-SWCNTs [7, 16–18], the perpendicularly polarized absorptions show dramatic effects of e–e interactions. Unlike in the S-SWCNTs, though, the lowest perpendicularly polarized absorptions will occur *below* the lowest longitudinal absorption in the M-SWCNTs. In section 4 we present our conclusions, focusing on the difference between our results and those obtained within the *ab initio* approach [41].

2. π-electron model and its parameterization

We investigate theoretically the photophysics of M-SWCNTs within the same π-electron Pariser–Parr–Pople (PPP) [42] model that we have used for the S-SWCNTs [7, 8] and planar π-conjugated polymers [43]:

$$H = -t\sum_{\langle ij\rangle,\sigma}(c^{\dagger}_{i,\sigma}c_{j,\sigma} + H.C.) + U\sum_{i} n_{i,\uparrow}n_{i,\downarrow} + \sum_{i<j} V_{ij}(n_i - 1)(n_j - 1) \quad (1)$$

where $c^{\dagger}_{i,\sigma}$ creates a π-electron of spin σ on carbon atom i, $n_{i,\sigma} = c^{\dagger}_{i,\sigma}c_{i,\sigma}$ is the number of electrons on atom i with spin σ and $n_i = \sum_{\sigma} n_{i,\sigma}$ is the total number of electrons on atom i. Here t is the nearest-neighbor one-electron hopping, and U and V_{ij} are the on-site and intersite Coulomb interactions. We parameterize V_{ij} as [7, 8, 43]

$$V_{ij} = \frac{U}{\kappa\sqrt{1 + 0.6117R^2_{ij}}} \quad (2)$$

where R_{ij} is the distance between carbon atoms i and j in ångströms and κ is the background dielectric constant. Since full many-body calculations are not possible within equation (1), we use the single-configuration interaction (SCI), which retains all matrix elements between single excitations from the Hartree–Fock (HF) ground state. Calculations reported below are for 60 or more unit cells, with open boundary conditions [7, 8].

The three independent parameters within equation (1) are t, U and κ. The nearest-neighbor hopping integral is widely accepted to be 2.4 eV in planar π-conjugated systems [43]. The hopping in SWCNTs is smaller because of the curvature, which decreases the overlaps between neighboring p_z orbitals. A smaller t of 2.0 eV for S-SWCNTs was determined from careful fitting of the experimental data [8]. Since the curvature effects in M-SWCNTs are the same as in S-SWCNTs, we use the same $t = 2.0$ eV as in the S-SWCNTs. Not surprisingly, the Hubbard on-site repulsion U is found to be the same in both π-conjugated polymers [43] and S-SWCNTs [7, 8, 17], namely 8 eV, which would place both these classes of materials among the strongly correlated-electron systems. In the context of a different class of 1D correlated-electron materials, organic charge-transfer solids, it has been shown by numerous authors in the past that the short-range e–e interaction, in particular the Hubbard U, remains practically unchanged between the $\frac{1}{2}$-filled band semiconductors and the non-$\frac{1}{2}$-filled conductors [44–48]. This conclusion has been substantiated by more recent work [49, 50] and is also in agreement with theories of high temperature superconductors, within which the undoped Mott–Hubbard semiconductors and the doped conductors and superconductors are generally assumed to have the same U. Based on prior work, we therefore expect the Hubbard U to be the same in M-SWCNTs and S-SWCNTs, and use $U = 8$ eV in our calculations reported here (see, however, below).

The long-range interaction V_{ij} in M-SWCNTs, however, can be different from S-SWCNTs due to screening, and this is taken into account by modifying κ. We arrive at the appropriate κ by comparing the experimental lowest longitudinal exciton energies in three different M-SWCNTs: (8, 8) armchair, (12, 0) zigzag and (9, 6) chiral with PPP-SCI energies, calculated using multiple values of κ. In table 1 we show our comparisons of the calculated and experimental quantities for the (8, 8), (12, 0) and (9, 6) M-SWCNTs. The two nonarmchair M-SWCNTs, in which E_{11} splits into a lower E^{-}_{11} and an upper E^{+}_{11} due to trigonal warping [36], provide rigorous tests of our theory. As seen in the table, while the κ appropriate for M-SWCNTs is certainly larger than the value of 2 used for S-SWCNTs [8], $\kappa > 3$ yields exciton energies that are too small. The only exception to this is E^{-}_{11} for the (12, 0) NT. Note, however, that (i) this is the narrowest NT considered (as has been emphasized in [8], π-electron theory becomes less quantitative for small d) and (ii) even here the best fit to E^{+}_{11} is with $\kappa = 3$. We have therefore chosen $\kappa = 3$ in what follows.

In the above, we have shown results for a fixed $U = 8$ eV, based on our previous work on the π-conjugated polymer poly(paraphenyelenevinylene), the optical absorption spectrum of which was fitted against calculated results obtained with four values of U and three values of κ [43]. Four different absorption bands are seen here, and only with $U = 8$ eV and $\kappa = 2$ could we fit all four bands. We have performed similar calculations for the (12, 0) NT with $U = 4$, 6 and 8 eV, and $\kappa = 2$ and 3. In all cases the discrepancies between the calculated and experimental E^{-}_{11} and E^{+}_{11} were much larger

Table 1. Calculated and experimental [36] exciton energies for three M-SWCNTs with $t = 2.0$ eV and $U = 8$ eV, and several different κ.

			E_{11}^{-} (eV)		E_{11}^{+} (eV)	
(n, m)	d (nm)	κ	PPP	Expt.	PPP	Expt.
(8, 8)	1.10	2.0	2.35	2.11	—	—
		2.2	2.26		—	
		3.0	2.07		—	
		3.5	2.00		—	
		4.0	1.94		—	
(12, 0)	0.95	2.0	2.57	2.16	2.71	2.47
		2.2	2.48		2.63	
		3.0	2.28		2.49	
		3.5	2.21		2.42	
		4.0	2.15		2.37	
(9, 6)	1.04	2.0	2.35	2.15	2.52	2.22
		2.2	2.30		2.45	
		3.0	2.14		2.25	
		3.5	2.08		2.17	
		4.0	2.03		2.12	

than with $U = 8$ eV and $\kappa = 3$, except for $U = 6$ eV and $\kappa = 3$, for which the calculated E_{11}^{-} was closer to experiment than in table 1, but the difference from experimental E_{11}^{+} is larger. Notably, the calculated exciton binding energy is very similar to that obtained with the parameters of table 1. Because of this we have not pursued calculations with these parameters any further.

Additional justification of our parameters comes from three considerations. First, previous theoretical works on M-SWCNTs have already emphasized weak screening of e–e interactions in M-SWCNTs [19–25]. Our determination that κ in M-SWCNTs is only slightly larger than that in S-SWCNTs agrees with the conclusion of [20] that fitting the charging energy in M-SWCNTs requires a relatively small dielectric constant. Second, in the case of S-SWCNTs, the PPP-SCI approach has provided the best agreement with experimental absolute exciton energies and exciton binding energies to date for nanotubes with $d \geqslant 1$ nm. The *maximum* difference between our previously calculated and experimental E_{11} for S-SWCNTs with diameters in this range is 0.05 eV, while for slightly narrower tubes with d between 0.75 and 1.0 nm, this difference is 0.1 eV [8]. Our calculated exciton binding energies of 0.4–0.3 eV for S-SWCNTs with $d \sim 0.8$–1.0 nm are within 0.04 eV of the experimental quantities on average [8]. Our calculated energies of absorptions polarized perpendicular to the NT axes for four different S-SWCNTs with $d \sim 1$ nm are also within 0.1 eV of experimental values [17].

Finally, we justify ignoring atomic orbitals other than the carbon p_z orbitals based on existing work and symmetry considerations. Within one-electron considerations alone [51], curvature effects are weak for SWCNTs with $d \geqslant 1$ nm, systems of interest here. The characterization of bands as approximately σ and π therefore persists for these diameters. Many-electron interactions can in principle promote mixing of HF excitations involving σ and π bands. The extent of configuration mixing depends on the *difference* in the HF energies of the configurations in question. This difference is close to zero between pairs of $\pi \rightarrow \pi^*$ excitations (it is exactly zero for the degenerate perpendicular excitations, CI between which is therefore very strong), but it can be very large between $\pi \rightarrow \pi^*$ excitations and excitations involving σ or σ^* bands. Furthermore, symmetry considerations preclude configuration mixing between $\pi \rightarrow \pi^*$ excitations and $\sigma \rightarrow \pi^*$ and $\pi \rightarrow \sigma^*$ excitations, and only the CI between $\pi \rightarrow \pi^*$ and $\sigma \rightarrow \sigma^*$ excitations is allowed. From the calculated first-principles band structure of the (6, 6) M-SWCNT, the σ–σ^* energy separation is ∼15 eV at the k-point where the π–π^* gap is the smallest, giving an energy difference of >12–13 eV relative to the $\pi \rightarrow \pi^*$ optical excitations [52]. This indicates that the mixing between $\pi \rightarrow \pi^*$ and $\sigma \rightarrow \sigma^*$ excitations is small.

Table 2. Calculated and experimental exciton energies in M-SWCNTs and the calculated binding energies of the excitons.

		E_{11}^{-} (eV)		E_{11}^{+} (eV)		E_{b1} (eV)
(n, m)	d (nm)	PPP	Expt.	PPP	Expt.[a]	PPP
(7, 7)	0.96	2.31	2.34[a], 2.43[b]	—	—	0.31
(8, 8)	1.10	2.07	2.11[a], 2.22[b]	—	—	0.28
(9, 9)	1.24	1.88	1.91[a], 2.03[b], 2.02[c]	—	—	0.25
(10, 10)	1.38	1.72	1.75[a], 1.89[b,c]	—	—	0.23
(10, 1)	0.84	2.51	2.33[a], 2.28[b], 2.38[c]	2.83	2.71	0.30
(9,3)	0.86	2.47	2.36[a], 2.35[b], 2.43[c]	2.71	2.61	0.29
(8,5)	0.90	2.42	2.37[a], 2.47[b,c]	2.54	2.47	0.29
(12, 0)	0.95	2.28	2.16[a,b]	2.49	2.47	0.27
(10,4)	0.99	2.22	2.17[a], 2.22[b]	2.37	2.33	0.27
(9, 6)	1.04	2.14	2.15[a], 2.23[b], 2.24[c]	2.25	2.22	0.27
(13, 1)	1.07	2.07	2.01[a], 2.02[b], 2.06[c]	2.26	2.24	0.25
(15, 0)	1.19	1.91	1.86[a,c], 1.88[b]	2.03	2.06	0.24

[a] from reference [36]; [b] from references [38] and [39]; [c] from reference [37].

3. Results

3.1. Linear and nonlinear absorptions in M-SWCNTs

In table 2 we present our calculated and experimental [36–39] absolute energies of the excitons for twelve different M-SWCNTs with $d > 0.8$ nm. We compare theoretical results mostly against the experimental results of [36], which is the only work that reports both E_{11}^{-} and E_{11}^{+} for the nonarmchair M-SWCNTs. We obtain excellent fits to experiments in all cases. Importantly, our calculations reproduce almost quantitatively the small energy differences between E_{11}^{-} and E_{11}^{+}. Our largest deviations, 0.18 eV for E_{11}^{-} and 0.12 eV for E_{11}^{+}, are for the (10, 1) NT with smallest d. Theoretical and experimental results agree particularly well for the (15, 0) and (13, 1) NTs, for which the experimental quantities reported in the different references are close.

Table 2 also lists our calculated binding energies E_{b1}, which we define as the energy difference between the lower threshold of the continuum band and the E_{11} (E_{11}^{-}) exciton in armchair (nonarmchair) M-SWCNTs. Within the SCI approximation, the Hartree–Fock threshold gives the threshold of the continuum [7, 8, 43]. The E_{b1} in all cases are significantly larger than those obtained within *ab initio*

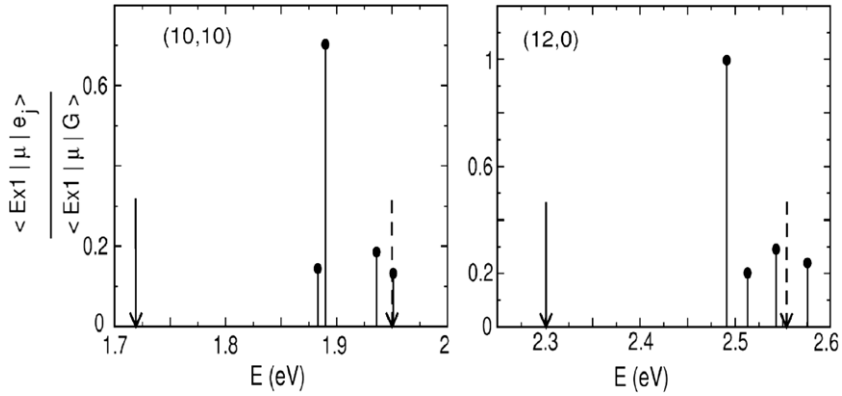

Figure 2. Transition dipole couplings between above-gap excited states j and the optical exciton Ex1, relative to the dipole coupling between Ex1 and the ground state G, in the (10, 10) and (12, 0) M-SWCNTs. The solid and dashed arrows denote the energy locations of the optical exciton and the threshold of the continuum band, respectively.

theory [41] and are 70–80% of the exciton binding energies in S-SWCNTs with similar diameters [8]. For M-SWCNTs with $d \sim 1$ nm, for instance, the *ab initio* work had predicted $E_{b1} \sim 0.05$ eV, while the PPP values are 0.25–0.30 eV. Our ability to reproduce the small energy differences between E_{11}^{-} and E_{11}^{+} gives us confidence about our calculated E_{b1}.

The predicted large E_{b1} can be verified from pump-probe measurements of excited state absorptions [11]. In figures 2(a) and (b) we show the calculated normalized transition dipole couplings between the lowest optical exciton and higher energy two-photon states in the (10, 10) and (12, 0) M-SWCNTs. As in the S-SWCNTs [11], there occurs a dominant two-photon exciton that is strongly dipole-coupled to the optical exciton and that therefore should be visible as excited state absorption. We find similar results in the other metallic NTs. The energy difference between the two-photon exciton and the optical exciton is the lower bound to E_{b1}.

3.2. Optical absorption in the (21, 21) M-SWCNT

The absorption spectrum in the E_{22} region of the (21, 21) M-SWCNT ($d = 2.9$ nm) has recently been obtained experimentally [40]. The absorption band is asymmetric, with weak but significant absorption on the high energy side of the peak in the absorption (see figure 3). Based on comparisons with the rigidly downshifted symmetric E_{44} absorption spectrum of the (16, 15) S-SWCNT and lineshape analysis, the authors of this work concluded that E_{b2} in (21, 21) M-SWCNT is only 0.05 eV. As an *ab initio* calculation for the wide (21, 21) M-SWCNT is difficult, the authors used the calculated *ab initio* E_{11} transition of the (10, 10) S-SWCNT ($d = 1.38$ nm) to fit the experimental E_{22} absorption of the (21, 21) M-SWCNT, since within band theory the two one-electron gaps have the same origin and are the same in magnitude (the absorptions to the exciton and the continuum band were, however, calculated separately and superimposed in this work). The *ab initio* E_{b1} of the (10, 10) M-SWCNT is also ∼0.05 eV, seemingly supporting the conjecture that the E_{11} exciton of the (10, 10) M-SWCNT and the E_{22} exciton of the (21, 21) M-SWCNT are equivalent even when e–e interactions

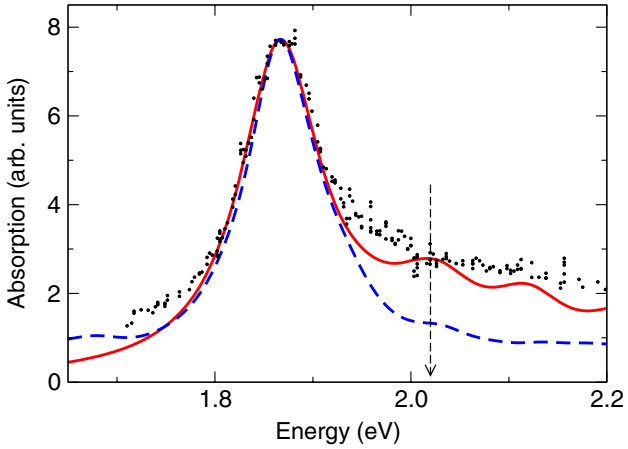

Figure 3. Calculated absorption spectrum (red curve) in the E_{22} region of the (21, 21) M-SWCNT, superimposed on the experimental data [40] (black dots). The calculated spectrum has been shifted rigidly by 0.12 eV. The arrow gives the calculated threshold of the continuum band. The blue dashed curve is the calculated E_{22} absorption of the (19, 0) S-SWCNT, shifted rigidly so that the peaks of the two calculated spectra match. Linewidths of 0.05 eV and 0.04 eV, respectively, for the (21, 21) and (19, 0) NTs, have been used.

(This figure is in colour only in the electronic version)

are significant. Note that our calculated E_{b1} in the (10, 10) M-SWCNT in table 2 is, however, significantly larger (0.23 eV), implying that substituting the E_{11} spectrum of the (10, 10) NT for the E_{22} spectrum of the (21, 21) NT may not be appropriate.

We have calculated directly the entire absorption spectrum in the E_{22} region of the (21, 21) M-SWCNT within a single calculation using the PPP-SCI approach. Comparison of the theoretical and experimental absorption spectra provides a direct test of our theory. Our calculated E_{22} is 1.75 eV, in good agreement with the experimental E_{22} of 1.87 eV [40]. The calculated exciton energy is indeed close to E_{11} in the (10, 10) M-SWCNT (see table 2). In figure 3 we compare our calculated absorption spectrum, rigidly shifted by the 0.12 eV energy difference between our calculated and experimental

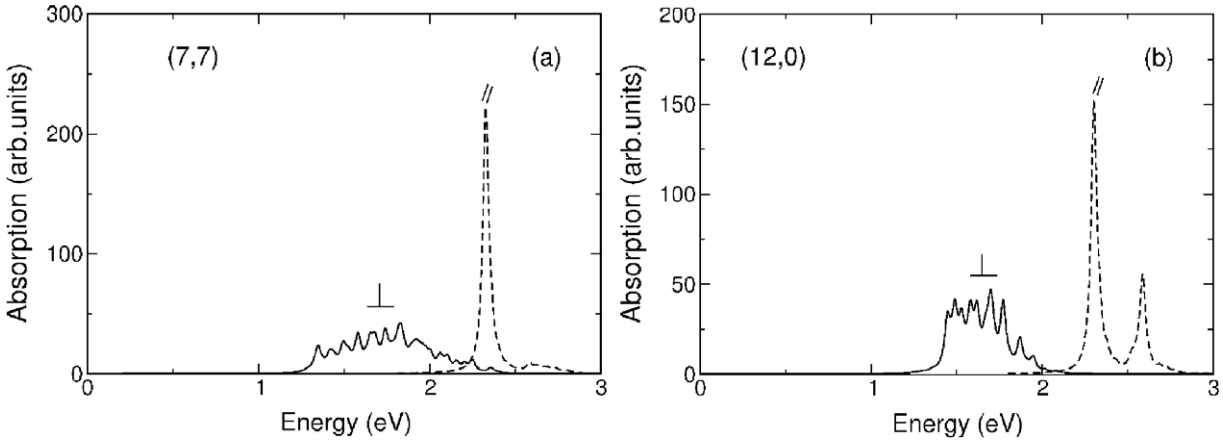

Figure 4. Calculated optical absorptions polarized perpendicular to the NT axes in the (a) (7, 7) and (b) (12, 0) M-SWCNTs. The E_{11} absorptions are included for comparison (the splitting of E_{11} in (b) is due to trigonal warping). The zero-frequency Drude absorptions are not shown.

E_{22}, with the experimental data points of [40]. Apart from this rigid shift, the fitting is excellent: the calculated spectrum reproduces both the asymmetric lineshape as well as the high energy tail. The latter is not due to absorption by the continuum band [41], but is due to weak absorptions to higher excitons that lie below the continuum band threshold. Similar absorptions to higher excitons are known to contribute to the asymmetric lineshapes of absorptions within the PPP Hamiltonian, whenever the exciton binding energy is relatively small [43] and occur also in the perpendicularly polarized absorptions in S-SWCNTs with $d \sim 1$ nm, where the transverse excitons have binding energies of 0.1–0.15 eV (see the experimental absorption spectra in figure 3(d) in [15] and the calculated absorption spectra in figure 3 of [17]). For comparison with the absorption to an exciton in a S-SWCNT, as was done in [40], we have superimposed in figure 3 the calculated absorption band in the E_{22} region of the (19, 0) S-SWCNT, again rigidly shifted such that the peaks of the two calculated absorptions match. According to the prescription of [40], the threshold of the E_{22} continuum of the (21, 21) M-SWCNT should occur at the energy where the absorptions of the semiconducting and the metallic NTs begin to diverge, namely at ∼1.92 eV from figure 1(c). The actual calculated threshold of the continuum, indicated by the arrow in figure 3, is, however, at a significantly higher energy. We calculate E_{b2} in the (21, 21) M-SWCNT to be 0.12 eV, nearly half that of the (10, 10) M-SWCNT.

For S-SWCNTs, E_{b1} and E_{b2} for the same system are comparable. Furthermore, exciton binding energies in S-SWCNTs decrease with diameter [7, 8]. If one assumes both of these to be true in M-SWCNTs, comparable E_{b2} in the (21, 21) M-SWCNT and E_{b1} in the (10, 10) M-SWCNT, as calculated within the *ab initio* theory, are not expected. The large difference between our calculated E_{b1} of 0.23 eV in the (10, 10) M-SCWNT (see table 2) and E_{b2} of 0.12 eV in the (21, 21) M-SCWNT, *in spite of the same absolute energies of the corresponding excitons*, in contrast, is in agreement with the diameter dependence in the semiconductors. The difference in the two binding energies is not surprising. The thresholds of the continua in our calculations correspond to the Hartree–Fock thresholds within equation (1). These energies are different for the (10, 10) and (21, 21) M-SWCNTs even though their tight-binding thresholds are nearly the same. Although the lowest excitations in the M-SWCNTs do not necessarily reflect the behavior of the higher energy excitations, it is interesting that the mapping suggested in [19] predicts a U_{eff} in the (21, 21) M-SWCNT that is half the U_{eff} in the (10, 10) M-SWCNT.

3.3. Perpendicularly polarized absorption in M-SWCNTs

We now make a verifiable prediction concerning optical absorption polarized perpendicular to the NT axes. The strong blueshift of the transverse absorption from the exact center of E_{11} and E_{22} in the S-SWCNTs [15] is due to e–e interactions [7, 16–18]. Degenerate basis functions reached by E_{12} and E_{21} excitations here from new correlated-electron eigenstates that are odd and even superpositions of these basis functions. The redshifted odd superposition is optically forbidden, while the blueshifted even superposition is optically allowed [7, 17]. We anticipate the degenerate perpendicularly polarized one-electron transitions in M-SWCNTs (see figure 1) to be also similarly split by e–e interactions, giving rise to a redshifted forbidden transition and a blueshifted allowed absorption. The novel feature here, however, is that the lowest perpendicularly polarized absorption is 'subgap', occurring below the lowest longitudinal optical absorption.

In figures 4(a) and (b) we have shown our calculated perpendicularly polarized absorptions for the (7, 7) and the (12, 0) M-SWCNTs, where we have also included the longitudinal E_{11} absorptions. The subgap perpendicularly polarized absorptions are blueshifted substantially from the exact midgap. In spite of this strong Coulomb effect, we find the binding energy of the perpendicular absorption in the M-SWCNTs to be nearly zero.

4. Conclusions

To conclude, M-SWCNTs are expected to exhibit optical behavior very similar to S-SWCNTs, with only slightly smaller exciton binding energies. We emphasize that, within the PPP Hamiltonian of equation (1), determining the absolute energy of the exciton and its binding energy are *not* different problems. In the limit of large U with only nearest-neighbor intersite e–e interaction V_1, for example, the exciton in a purely 1D system occurs at energy $U - V_1$ while the conduction band is centered at U [53]. *Thus, in this limit, once the U is fixed, it is not possible to obtain the precise exciton energy but incorrect exciton binding energy.* For moderate U, where the hopping term plays a stronger role, it is necessary to also fix the t; but once again, for fixed U and t, correct determination of the absolute exciton energy within equation (1) necessarily implies that the continuum band threshold has also been correctly evaluated. Based on our argument in section 1 that the atomic U is the same in the S-SWCNTs and the M-SWCNTs then the excellent fits to the absolute exciton energies in table 2, as well as to the optical absorption spectrum in figure 3, imply that our estimates of the exciton binding energies are correct. The large E_b implies weak screening of Coulomb interactions. As we have pointed out, weak screening of e–e interactions in these 1D materials [19–25] suggests that simple concepts of metallic screening do not apply.

The discrepancy between the predictions of the molecular model used here and the *ab initio* approach is not unexpected. Note that, even for the S-SWCNTs, the calculated exciton binding energies within the two methods are widely different, with the *ab initio* approach predicting binding energies [4] that are often twice the experimental values [13]. Although it has been suggested that the experimental binding energies reflect screening of e–e interactions due to intertube interactions, and the true single-tube binding energies are much larger and close to the *ab initio* predictions, an alternate possibility is that the molecular model, which reproduces experimental longitudinal *and* transverse exciton energies and exciton binding energies quantitatively, is simply better calibrated to handle systems with large Hubbard interaction. The difficulty of treating strong on-site e–e interaction within density functional based theories, for instance, is well known [54–56].

SWCNTs are currently of great interest because of their potential technological applications. Our demonstration that M-SWCNTs will exhibit photophysics similar to the semiconductors, even as their transport behavior corresponds to that of unconventional conductors, may introduce new and exciting possibilities.

Acknowledgments

We are grateful to Professors F Wang and T F Heinz for sending us the experimental absorption data for the (21, 21) NT, and to Professors A Shukla and Z V Vardeny for critical reading of the manuscript. This work was supported by NSF grant no. DMR-0705163.

References

[1] Ando T 1997 *J. Phys. Soc. Japan* **66** 1066
[2] Lin M F 2000 *Phys. Rev.* B **62** 13153
[3] Kane C L and Mele E J 2003 *Phys. Rev. Lett.* **90** 207401
[4] Spataru C D, Ismail-Beigi S, Benedict L X and Louie S G 2004 *Phys. Rev. Lett.* **92** 077402
[5] Chang E, Bussi G, Ruini A and Molinari E 2004 *Phys. Rev. Lett.* **92** 196401
[6] Perebeinos V, Tersoff J and Avouris Ph 2004 *Phys. Rev. Lett.* **92** 257402
[7] Zhao H and Mazumdar S 2004 *Phys. Rev. Lett.* **93** 157402
[8] Wang Z, Zhao H and Mazumdar S 2006 *Phys. Rev.* B **74** 195406
[9] Dresselhaus M S, Dresselhaus G, Saito R and Jorio A 2007 *Annu. Rev. Phys. Chem.* **58** 719
[10] Scholes G D, Tretiak S, McDonald T J, Metzger W K, Engtrakul C, Rumbles G and Heben M J 2007 *J. Phys. Chem.* C **111** 11139
[11] Zhao H, Mazumdar S, Sheng C-X, Tong M and Vardeny Z V 2006 *Phys. Rev.* B **73** 075403
[12] Wang F, Dukovic G, Brus L E and Heinz T F 2005 *Science* **308** 838
[13] Dukovic G, Wang F, Song D, Sfeir M Y, Heinz T F and Brus L E 2005 *Nano Lett.* **5** 2314
[14] Maultzsch J *et al* 2005 *Phys. Rev.* B **72** 241402(R)
[15] Miyauchi Y, Oba M and Maruyama S 2006 *Phys. Rev.* B **74** 205440
[16] Uryu S and Ando T 2006 *Phys. Rev.* B **74** 155411
[17] Wang Z, Zhao H and Mazumdar S 2007 *Phys. Rev.* B **76** 115431
[18] Kilina S, Tretiak S, Doorn S K, Luo Z, Papadimitrakopoulos F, Piryatinski A, Saxena A and Bishop A R 2008 *Proc. Natl Acad. Sci.* **105** 6797
[19] Balents L and Fisher M P A 1997 *Phys. Rev.* B **55** R11973
[20] Egger R and Gogolin A O 1997 *Phys. Rev. Lett.* **79** 5082
[21] Kane C, Balents L and Fisher M P A 1997 *Phys. Rev. Lett.* **79** 5086
[22] Krotov Y A, Lee D H and Louie S G 1997 *Phys. Rev. Lett.* **78** 4245
[23] Yoshioka H and Odintsov A A 1999 *Phys. Rev. Lett.* **82** 374
[24] Odintsov A A and Yoshioka H 1999 *Phys. Rev.* B **59** R10457
[25] Bunder J E and Lin H-H 2007 *Phys. Rev.* B **75** 075418
[26] Tans S J, Devoret M H, Dai H, Thess A, Smalley R E, Geerligs L J and Dekker C 1997 *Nature* **386** 474
[27] Tans S J, Devoret M H, Groeneveld R J O and Dekker C 1998 *Nature* **394** 761
[28] Bockrath M, Cobden D H, McEuen P L, Chopra N G, Zettl A, Thess A and Smalley R E 1997 *Science* **275** 1922
[29] Bockrath M, Cobden D H, Rinzler A G, Smalley R E, Balents L and McEuen P L 1999 *Nature* **397** 598
[30] Dagotto E and Rice T M 1996 *Science* **271** 618
[31] Soos Z G, Ramasesha S and Galvao D S 1993 *Phys. Rev. Lett.* **71** 1609
[32] Tretiak S 2007 *Nano Lett.* **7** 2201
[33] Singer P M, Wzietek P, Alloul H, Simon F and Kuzmany H 2005 *Phys. Rev. Lett.* **95** 256403
[34] Likodimos V, Glenis S, Guskos N and Lin C L 2007 *Phys. Rev.* B **76** 075420
[35] Imai H, Babu P K, Oldfield E, Wieckowski A, Kasuya D, Azami T, Shimakawa Y, Yudasaka M, Kubo Y and Iijima S 2006 *Phys. Rev.* B **73** 125405
[36] Strano M S *et al* 2003 *Nano Lett.* **3** 1091
[37] Telg H, Maultzsch J, Reich S, Hennrich F and Thomsen C 2004 *Phys. Rev. Lett.* **93** 177401
[38] Fantini C, Jorio A, Souza M, Strano M S, Dresselhaus M S and Pimenta M A 2004 *Phys. Rev. Lett.* **93** 147406
[39] Fantini C, Jorio A, Santos A P, Peressinotto V S T and Pimenta M A 2007 *Chem. Phys. Lett.* **439** 138

[40] Wang F *et al* 2007 *Phys. Rev. Lett.* **99** 227401
[41] Deslippe J, Spataru C D, Prendergast D and Louie S G 2007 *Nano Lett.* **7** 1626
[42] Pariser R and Parr R G 1953 *J. Chem. Phys.* **21** 466
Pople J A 1953 *Trans. Faraday Soc.* **49** 1375
[43] Chandross M and Mazumdar S 1997 *Phys. Rev.* B **55** 1497
[44] Soos Z G 1974 *Annu. Rev. Phys. Chem.* **25** 121
[45] Torrance J B 1979 *Acc. Chem. Res.* **12** 79
[46] Hubbard J 1978 *Phys. Rev.* B **17** 494
[47] Mazumdar S and Bloch A N 1983 *Phys. Rev. Lett.* **50** 207
[48] Mazumdar S and Dixit S N 1986 *Phys. Rev.* B **34** 3683
[49] Claessen R, Sing M, Schwingenschlogl U, Blaha P, Dressel M and Jacobsen C S 2002 *Phys. Rev. Lett.* **88** 096402
[50] Bozi D, Carmelo J M P, Penc K and Sacramento P D 2008 *J. Phys.: Condens. Matter* **20** 022205
[51] Saito R, Dresselhaus G and Dresselhaus M S 1998 *Physical Properties of Carbon Nanotubes* (Singapore: Imperial College Press)
[52] Reich S, Thomsen C and Ordejon P 2002 *Phys. Rev.* B **65** 155411
[53] Guo D, Mazumdar S, Dixit S N, Kajzar F, Jarka F, Kawabe Y and Peyghambarian N 1993 *Phys. Rev.* B **48** 1433
[54] Kotliar G, Savrasov S Y, Haule K, Oudovenko V S, Parcollet P and Marianetti C A 2006 *Rev. Mod. Phys.* **78** 865
[55] Savrasov S Y, Kotliar G and Abrahams E 2001 *Nature* **410** 793
[56] Cohen A J, Mori-Sánchez P and Yang W 2008 *Science* **321** 792